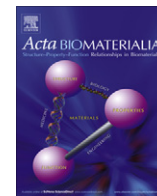




Contents lists available at SciVerse ScienceDirect

Acta Biomaterialia

journal homepage: www.elsevier.com/locate/actabiomat

Fabrication and characterization of monodisperse PLGA–alginate core–shell microspheres with monodisperse size and homogeneous shells for controlled drug release

Qi Jun Wu^a, Tiantian Kong^b, Kelvin Wai Kwok Yeung^a, Ho Cheung Shum^{b,c}, Kenneth Man Chee Cheung^a, Liqiu Wang^{b,d}, Michael Kai Tsun To^{a,*}

^a Department of Orthopaedics and Traumatology, Li Ka Shing Faculty of Medicine, The University of Hong Kong, Hong Kong

^b Department of Mechanical Engineering, Faculty of Engineering, The University of Hong Kong, Hong Kong

^c HKU-Shenzhen Institute of Research and Innovation (HKU-SIRI), Shenzhen, Guangdong, China

^d Lab for Nanofluids and Thermal Engineering, Zhejiang Institute of Research and Innovation, The University of Hong Kong, Hong Kong

ARTICLE INFO

Article history:

Received 2 November 2012

Received in revised form 21 February 2013

Accepted 18 March 2013

Available online xxx

Keywords:

PLGA

Core–shell microspheres

Capillary microfluidic device

Controlled drug release

ABSTRACT

Monodisperse PLGA–alginate core–shell microspheres with controlled size and homogeneous shells were first fabricated using capillary microfluidic devices for the purpose of controlling drug release kinetics. Sizes of PLGA cores were readily controlled by the geometries of microfluidic devices and the fluid flow rates. PLGA microspheres with sizes ranging from 15 to 50 μm were fabricated to investigate the influence of the core size on the release kinetics. Rifampicin was loaded into both monodisperse PLGA microspheres and PLGA–alginate core–shell microspheres as a model drug for the release kinetics studies. The in vitro release of rifampicin showed that the PLGA core of all sizes exhibited sigmoid release patterns, although smaller PLGA cores had a higher release rate and a shorter lag phase. The shell could modulate the drug release kinetics as a buffer layer and a near-zero-order release pattern was observed when the drug release rate of the PLGA core was high enough. The biocompatibility of PLGA–alginate core–shell microspheres was assessed by MTT assay on L929 mouse fibroblasts cell line and no obvious cytotoxicity was found. This technique provides a convenient method to control the drug release kinetics of the PLGA microsphere by delicately controlling the microstructures. The obtained monodisperse PLGA–alginate core–shell microspheres with monodisperse size and homogeneous shells could be a promising device for controlled drug release.

© 2013 Acta Materialia Inc. Published by Elsevier Ltd. All rights reserved.

1. Introduction

The development of modern therapeutics has raised the requirement for controlled drug delivery devices which can release drugs at a predetermined rate for a long time [1]. Controlled drug release offers numerous advantages over conventional drugs (free drugs) [2], such as improved efficacy, reduced side-effects and improved patient compliance [3–5]. Currently, the widely used controlled drug delivery devices include nanoparticles and microparticles made from polymers and liposomes [6–9]. The majority of such devices have been facing the challenges of broad size distribution, high initial burst release and uncontrollable drug release kinetics. Recent reports have suggested that the shape and size of drug delivery devices have significant impacts on the initial burst effect and the drug release kinetics [10–13]. Therefore, fabricating monodisperse nano/microparticles with controlled size and shape

has become one of the key issues in developing controlled drug delivery devices.

To date, only a few technologies have been found to be inherently suitable for fabricating monodisperse nano/microparticles with controlled size. Microfluidics, which is a group of technologies involved in the manipulation of fluids using channels in the scale of micrometers [14,15], is of particular interests due to its ability to control the size and the shape of droplets [16–19]. Great effort has been made to investigate the ability of microfluidics in fabricating monodisperse drug delivery devices with controlled microstructure [20,21]. Recently, monodisperse PLGA microparticles were fabricated using microfluidic devices [22]. The authors found that monodisperse microparticles fabricated using microfluidic devices exhibited slower overall release rate and reduced initial burst release, compared with conventional polydisperse PLGA microparticles of similar average diameters. More recently, microfluidics was also applied in the fabrication of monodisperse porous PLGA microspheres with tunable pore size [23]. Although some achievements have been made, systematical studies of the relationships

* Corresponding author. Tel.: +852 29740274; fax: +852 29740621.

E-mail address: mikekto@hku.hk (M.K.T. To).

between the size and the drug release kinetics of monodisperse microparticles are far from complete.

Rifampicin-PLGA microspheres entrapped in alginate hydrogel matrix showed significantly prolonged drug release duration compared with bare rifampicin-PLGA microspheres [24]. Core-shell microcapsules made of PLGA and alginate were fabricated with a coaxial electro-dropping method [25]. Using the core-shell microcapsules, dual drug release was achieved and the initial burst was highly suppressed when the biomolecule was loaded in the PLGA core. However, fabricating homogeneous shells and controlling the size of microparticles in a convenient and energy-saving way remain difficult. The microfluidic method is a promising candidate for fabricating homogeneous core-shell microspheres with controlled size because of its ability to delicately control the size and the structure of droplets in the microscale. Although core-shell emulsions have been generated by microfluidics [26], their applications in drug delivery are limited due to the instability of liquid. In this study, monodisperse PLGA-alginate core-shell microspheres composed of a single PLGA microspheric core and a homogeneous alginate shell were fabricated using a capillary microfluidic device for the purpose of controlling the drug release kinetics. PLGA was chosen as the drug carrier for its excellent biocompatibility. Its readily variable degradation rate ranging from 1 to 5 months can meet the requirements of most biomedical applications. Alginate was used as the shell material to modulate the drug release profile. Alginate has found numerous applications in drug delivery for its biocompatibility and ease of gelation [27,28]. Nevertheless, other biocompatible polymers and polysaccharides can also be processed using the capillary microfluidic system presented in this study. The selection of the materials mainly depends on the requirements imposed by the biomedical application. Rifampicin was loaded in the PLGA core as a model drug. The size of PLGA-alginate core-shell microspheres was well controlled by varying the fluid flow rates and the geometries of capillary microfluidic devices. Monodisperse PLGA microspheres with four different diameters were also fabricated using capillary microfluidic devices to study the effect of the core size on the drug release kinetics. The drug content, encapsulation efficiency and in vitro release profiles exhibited by these drug delivery devices were subsequently compared. Structures and surface morphologies were observed by microscopy and scanning electron microscopy (SEM). Biocompatibility of the PLGA-alginate core-shell microspheres was evaluated by cell viability from MTT assay. The present technique provides a method to fabricate monodisperse

core-shell microspheres with controllable size and homogeneous shells which can be applied in controlled drug release.

2. Materials and methods

2.1. Materials

PLGA (L/G = 50:50, Mw = 7000–17,000) was purchased from Aldrich. Alginate in the form of alginic acid sodium salt was purchased from Fluka. Poly(vinyl alcohol) (PVA, 87–89% hydrolyzed, Mw = 13,000–23,000 Da) and anhydrous calcium chloride were obtained from Sigma-Aldrich. Rifampicin and phosphate-buffered saline (PBS, pH 7.4) was purchased from Sigma. All other chemicals and reagents were of analytical reagent grade. All reagents were used as received.

2.2. Fabrication of monodisperse PLGA microspheres with different diameters

PLGA microspheres were fabricated using a template of an oil-in-water single emulsion generated in capillary microfluidic devices [15,29]. The microfluidic devices were assembled as described below. Typically, two cylindrical capillaries (inner diameter/outer diameter: 0.58 mm/1 mm) were tapered by a micropipette puller (P-97, Sutter Instrument, Inc.). The tips of the capillaries were then polished to desired diameters using sandpaper. The tapered round capillaries were coaxially aligned inside a square capillary. The generation of PLGA single emulsion droplets is illustrated in Fig. 1a. The PLGA solution dissolved in dichloromethane (DCM; 8%, w/v) containing 0.8% (w/v) rifampicin was the inner oil phase. The aqueous PVA solution (1%, w/v) was the outer water phase. The inner phase flowed through the round capillary with a smaller nozzle diameter, known as the injection tube. The outer water phase flowed through the region between the injection tube and the outer square capillary. PLGA droplets were formed in the orifice of the remaining capillary, known as the collection tube. The PLGA emulsion droplets were collected with 0.1% (w/v) aqueous PVA solution in a beaker, and it usually takes 24 h to evaporate the DCM at room temperature without stirring. The obtained PLGA microspheres were washed with a large amount of deionized water and dried at 40 °C. The size of PLGA microspheres was controlled by the fluid flow rate and/or the diameter of the collection tube.

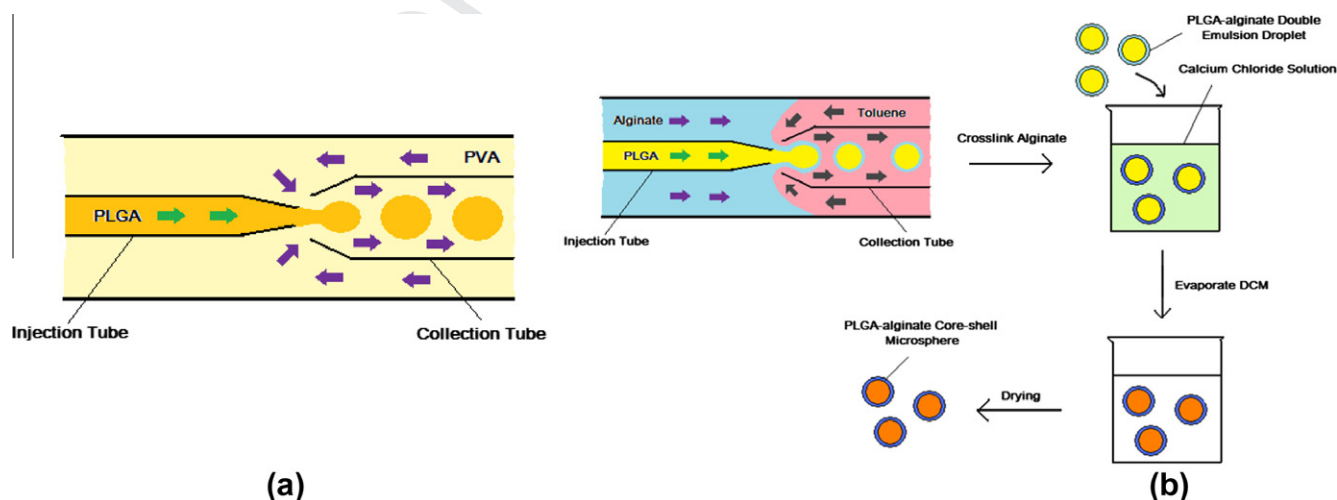


Fig. 1. Fabrication of PLGA microspheres and PLGA-alginate core-shell microspheres: (a) schematic diagram of PLGA single emulsion generation and (b) fabrication process of PLGA-alginate core-shell microspheres.

2.3. Fabrication of PLGA–alginate core–shell microspheres

The PLGA–alginate core–shell microspheres were fabricated using a similar capillary microfluidic device with small modifications for generating an oil-in-water-in-oil double emulsion as a template [15,29]. The injection tube was inserted into the collection tube. The inner surface of collection tube was rendered hydrophobic by dipping the collection tube into n-octadecyltrimethoxy silane and drying subsequently. The outer surface of the injection tube was gently wiped with a cotton swab soaked with hydrofluoric acid to make it more hydrophilic.

The fabrication process of PLGA–alginate core–shell microspheres is illustrated in Fig. 1b. First, fluids of three phases were guided into the microfluidic device as shown in Fig. 1b to generate PLGA–alginate double emulsion droplets. The PLGA solution in DCM (8%, w/v) containing 0.8% (w/v) rifampicin, the PVA solution (1%, w/v) containing 0.5% (w/v) alginate and the toluene containing 10% (w/w) span80 were used as the inner oil phase, middle aqueous phase and outer oil phase, respectively. Second, the double emulsion droplets were collected in a beaker containing calcium chloride solution to cross-link the alginate shell layer. Last, the droplets with hardened shells were left until complete evaporation of DCM at room temperature had occurred. The obtained PLGA–alginate microspheres were washed with distilled water and dried at 40 °C.

2.4. Characterization of PLGA microspheres and PLGA–alginate core–shell microspheres

The molecular structures of PLGA microspheres and PLGA–alginate core–shell microspheres were certificated by Fourier transform infrared (FTIR) transmission spectra (Perkin Elmer model 16PC). Microspheres were pressed into pellets with potassium bromide for the FTIR test. Morphologies and structures of PLGA microspheres and PLGA–alginate core–shell microspheres were characterized by SEM and microscopy. The SEM images were obtained using a variable pressure (VP) SEM (Hitachi S-3400N, Electron Microscope Unit, The University of Hong Kong). PLGA microspheres were coated with a thin layer of gold before observation. To obtain SEM images of PLGA–alginate core–shell microspheres, samples were directly observed without dehydration or coating in order to preserve as much original morphology of the alginate shells as possible. The observation was carried out under 120 Pa at –21 °C on a cooling stage. The mean diameters and the size distributions of PLGA microspheres and the PLGA cores of PLGA–alginate core–shell microspheres were determined by measuring at least 200 particles in the SEM image [30].

PLGA microspheres and PLGA–alginate core–shell microspheres were also observed using a microscope (Nikon Eclipse 80i) equipped with a digital camera (Nikon DXM1200F). Samples were dispersed in distilled water and spread on a glass slide. To visualize the transparent alginate shell, PLGA–alginate core–shell microspheres were stained with alcian blue (pH 1).

2.5. Drug content and encapsulation efficiency

The drug content of PLGA microspheres loaded with rifampicin was determined by lysing a certain amount of PLGA microspheres in 1 ml of 5% (w/v) sodium dodecyl sulfate solution containing 0.1 M sodium hydroxide [31]. The concentration of rifampicin in the supernatant was assayed by the UV method at 473 nm [32] with a microplate reader. For PLGA–alginate core–shell microspheres, the shells were removed by immersing the core–shell microspheres in 50 mM ethylenediaminetetraacetic acid solution before determining the drug content. The drug content of the microspheres and the core–shell microspheres was defined as the

weight percentage of rifampicin loaded in PLGA microspheres. Encapsulation efficiency was defined as the ratio of the actual amount of encapsulated rifampicin over the total amount of rifampicin used.

2.6. In vitro drug release

A certain amount of rifampicin loaded PLGA microspheres and PLGA–alginate core–shell microspheres was dispersed in 1 ml of PBS (pH 7.4) in centrifuge tubes and incubated at 37 °C. At each predetermined time interval, dispersions were briefly centrifuged and 200 µl of the supernatants was collected. The supernatants were then filtered and assayed by the UV method at 473 nm [32] with a microplate reader. PBS was replaced with fresh liquid at each time point after assaying the rifampicin. The first day's release was measured to investigate the burst effect. After that, measurement was carried out every 3 days. Unloaded PLGA microspheres were used as control.

2.7. Biocompatibility

The biocompatibility of PLGA–alginate core–shell microspheres was assessed by MTT assay according to ISO 10993-5 [33,34]. Extracts of the samples were prepared as described below [35]. In brief, 0.1 g ml⁻¹ PLGA–alginate core–shell microspheres in culture medium were incubated at 37 °C for 24 h. The extracts were filtered through a 0.2 µm membrane.

L929 mouse connective tissue fibroblast cell line (ATCC) was cultured in Dulbecco's modified Eagle's medium (DMEM) supplemented with 10% fetal bovine serum, 2 mM glutamine, 100 units ml⁻¹ penicillin and 100 µg ml⁻¹ streptomycin. Cell cultures were cultivated in tissue culture flasks and incubated in an incubator at 37 °C, 95% RH and 5% CO₂. The culture media were changed every other day.

L929 cells were harvested with 0.25% trypsin when cell monolayers reached more than 80% confluence. After that, cells were seeded in 96-well plates at a density of 5000 cells per well with 200 µl DMEM per well. After 24 h of incubation at 37 °C, the culture media were replaced with serial dilutions of the extracts. After 24 and 96 h, the cell viability was evaluated by MTT assay. In control wells, the culture media were replaced with fresh ones.

MTT (3-(4,5-dimethylthiazol-2-yl)-2,5-diphenyl tetrazolium bromide) was dissolved in PBS at 1 mg ml⁻¹ and filtered through a 0.2 µm membrane. To each well, 20 µl of the MTT stock was added, and the plates were wrapped in tin foil and incubated at 37 °C for another 4 h. Then the unreacted dye was aspirated, and the purple formazan products were dissolved in 200 µl per well of dimethyl sulfoxide and assayed at wavelengths of 570 and 690 nm (reference). The relative cell viability (%) related to control wells was calculated by $[\text{Absorbance}]_{\text{test}} / [\text{Absorbance}]_{\text{control}} \times 100$.

2.8. Statistical analysis

All tests were run in triplicate and data are presented as the mean ± standard deviation (SD). Statistical analyses were carried out by one-way analysis of variance using the SPSS software. Differences were considered to be statistically significant at a level of $p < 0.05$.

3. Results and discussion

3.1. Generation of PLGA droplets and PLGA–alginate double emulsion droplets

In order to control the size of PLGA microspheres, collection tubes with different diameters were used to assemble the capillary

microfluidic devices denoted as S1, S2 and S3. The PLGA-alginate double emulsion droplets were generated using a specifically designed capillary microfluidic device denoted as S4. The outer surface of the injection tube was rendered hydrophilic so that the aqueous middle phase adheres to the surface. As a result, it is easy for the middle phase to enter the collection tube and form a shell around the inner droplets.

The sizes of PLGA droplets and the core size of PLGA-alginate double emulsion droplets were obtained by measuring the diameter of droplets in the middle of the collection tube along the horizontal direction. The results are given in Table 1.

Basically, at fixed fluid flow rates (S1 and S3), increasing the tip diameter of the collection tube will result in bigger droplets. Similarly, the droplet size can also be increased by decreasing the flow rate of the outer phase while keeping other parameters unchanged (S2a and S2b). The core size of PLGA-alginate double emulsion droplets was also controlled by the fluid flow rates. By delicately selecting the flow rate of each phase, the core size of PLGA-alginate double emulsion droplets was adjusted to $\sim 80 \mu\text{m}$, which was the same as the PLGA droplet size of S3.

3.2. Structures and surface morphologies of PLGA microspheres and PLGA-alginate core-shell microspheres

As shown in Fig. 2, the FTIR spectrum of PLGA microspheres was similar to the reported data [36,37]. The peak at 1049 cm^{-1} was attributed to the C-CH₃ stretching vibration. The peak at 1084 cm^{-1} was due to the C-O-C stretching vibration. The peak at 1455 cm^{-1} was attributed to the C-H stretching in methyl groups. The characteristic peak of PLGA at 1740 cm^{-1} was due to the ester group. From the FTIR spectrum of PLGA-alginate core-shell microspheres, peaks assigned to PLGA were also observed. Because the peaks of alginate have been partially overlapped by the PLGA, only strong peaks of alginate can be found in the FTIR spectrum of core-shell microspheres. The most useful characteristic band of alginate at 1604 cm^{-1} was due to the C-O-O asymmetric stretching vibration. The broad peak around 3300 cm^{-1} was assigned to the O-H stretching vibration [38].

PLGA microspheres and PLGA-alginate core-shell microspheres were obtained by solidifying PLGA droplets and PLGA-alginate double emulsion droplets respectively. The structures and the surface morphologies of PLGA microspheres and PLGA-alginate core-shell microspheres were observed by microscopy (Fig. 3) and SEM (Fig. 4). According to the microscope images, PLGA microspheres fabricated by microfluidic method were homogeneous and have tunable diameters. The yellow color of PLGA microspheres indicated the successful encapsulation of rifampicin. The structure of PLGA-alginate core-shell microspheres was confirmed by the microscope images (Fig. 3e and f). To visualize the transparent alginate shell, alcian blue staining was applied. As shown in Fig. 3f, core-shell microspheres were composed of single PLGA cores with well controlled diameter and homogeneous alginate shells.

The mean diameters and the size distributions of PLGA microspheres and PLGA cores of PLGA-alginate core-shell microspheres were determined by measuring at least 200 particles in the SEM

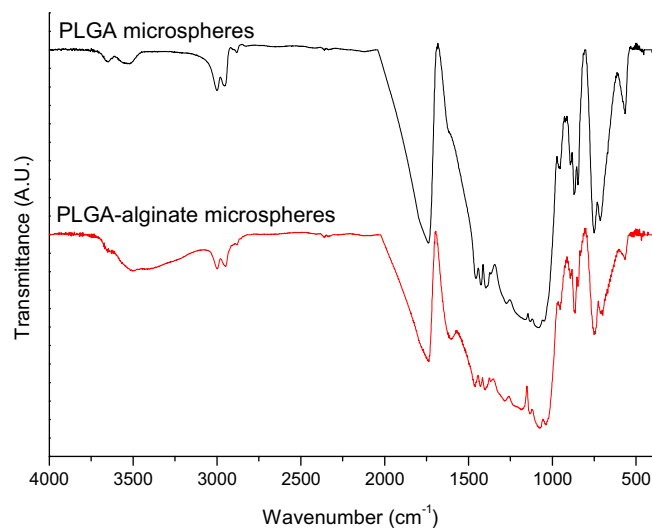


Fig. 2. FTIR spectra of PLGA microspheres and PLGA-alginate core-shell microspheres.

image [30]. The mean diameters are given in Table 2. The size distributions are shown in Fig. 5. Due to the shrinkage during the evaporation of DCM, the sizes of the microspheres were smaller than that of the droplets. However, the results confirmed that PLGA microspheres and PLGA-alginate core-shell microspheres were monodisperse. The diameters of PLGA microspheres and PLGA cores were readily controlled and ranged from ~ 15 to $\sim 55 \mu\text{m}$. VP SEM is a powerful tool to observe structures containing water such as the alginate shell in this study. The homogeneous core-shell structure was also confirmed by VP SEM imaging (Fig. 4e). SEM images further indicated that the surface morphologies of PLGA microspheres were influenced by the diameter of microspheres. Smaller PLGA microspheres exhibited smoother surface while larger microspheres have more surface pores. The surface pores formed during the evaporation of DCM. Larger microspheres had a relatively smaller surface-to-volume ratio so that the evaporation rates were slower. Therefore, larger microspheres took a longer time to solidify and underwent more severe deformation, which might result in more surface pores.

The microstructure of controlled drug delivery devices plays important roles in drug release kinetics. Conventional fabrication methods usually make nano/microparticles with broad size distribution. The microscope and SEM results demonstrated that PLGA microspheres and PLGA-alginate core-shell microspheres fabricated by capillary microfluidic method were monodisperse. The sizes of the PLGA microspheres and PLGA cores were readily controlled by the fluid flow rates and the geometry of capillary microfluidic devices. Furthermore, PLGA-alginate core-shell microspheres fabricated using capillary microfluidic devices exhibited homogeneous shells, which may facilitate the control of drug release kinetics. Therefore, monodisperse PLGA microspheres and PLGA-alginate core-shell microspheres fabricated by the capillary microfluidic method may be promising devices for controlled drug delivery.

Table 1
Parameters for generating PLGA droplets and PLGA-alginate double emulsion droplets.

No. of droplets	Microfluidic devices	Injection tube (μm)	Collection tube (μm)	Inner phase ($\mu\text{l h}^{-1}$)	Outer phase ($\mu\text{l h}^{-1}$)	Droplet size (μm)
S1	S1	20	63	800	6000	≈ 20
S2a	S2	20	99	800	8000	≈ 40
S2b	S2	20	99	800	2000	≈ 60
S3	S3	20	180	800	6000	≈ 80
S4	S4	20	180	Inner: 450, middle: 400, outer: 5000		≈ 80 (core)

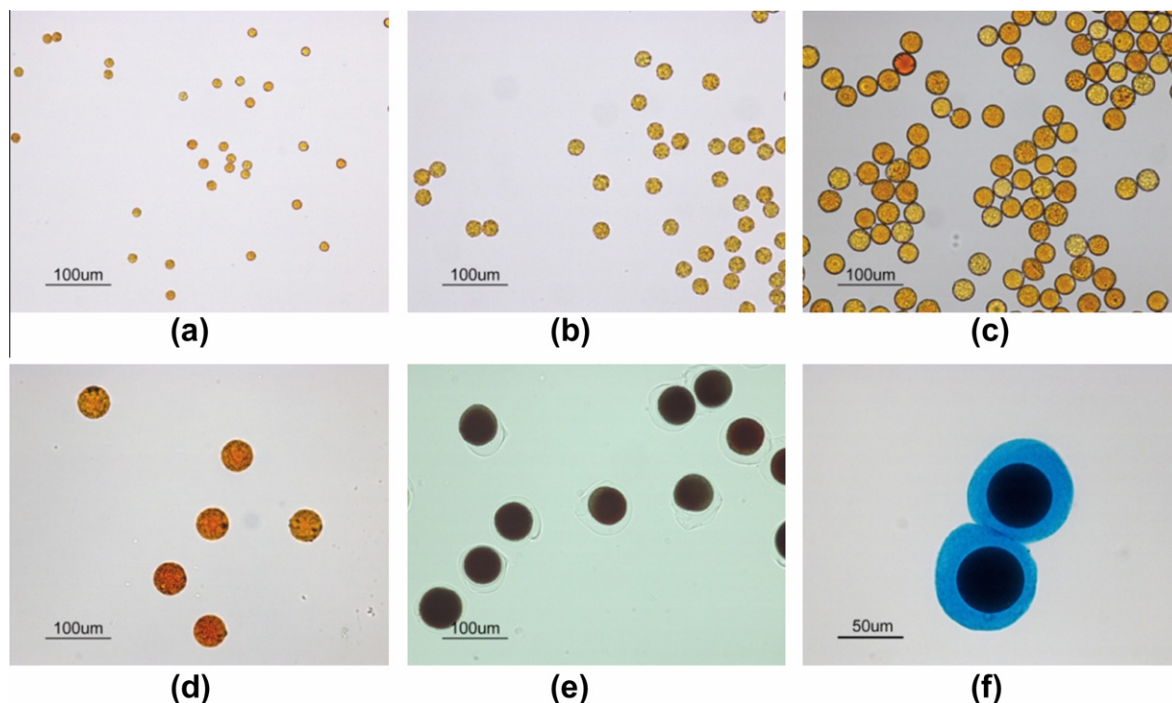


Fig. 3. Microscopic images of PLGA microspheres with diameters of 15 μm (a), 23 μm (b), 34 μm (c) and 49 μm (d). The PLGA core diameter of PLGA–alginate core–shell microspheres was $\sim 55 \mu\text{m}$ (e). After alcian blue staining, the alginate shell showed a blue color (f).

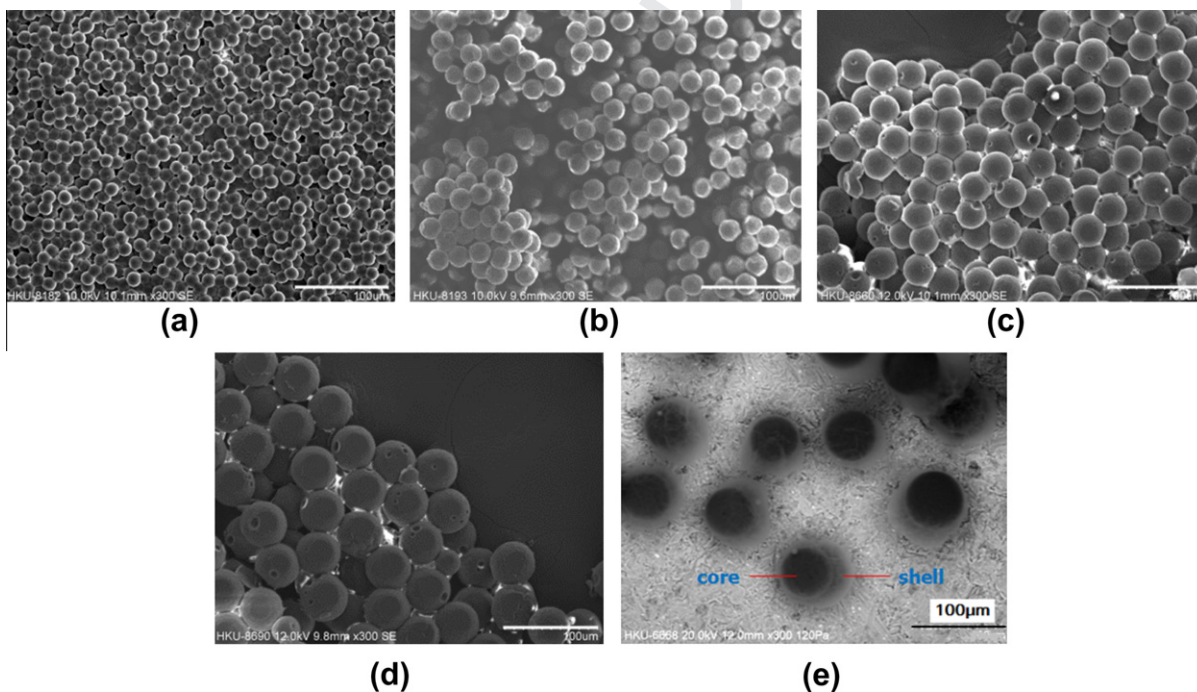


Fig. 4. SEM images of PLGA microspheres: (a) S1, 15 μm , (b) S2a, 23 μm , (c) S2b, 34 μm and (d) S3, 49 μm . PLGA–alginate core–shell microspheres: (e) S4, the diameter of PLGA core was 55 μm . The scale is 100 μm .

Table 2
Mean diameters of PLGA microspheres and PLGA cores.

	No.				
	S1	S2a	S2b	S3	S4 (core)
Size (μm)	15.2	23.6	34.2	49.2	55.1
SD	0.7	0.9	1.7	1.6	4.5

3.3. Influences of the size on the drug release kinetics

Monodisperse PLGA microspheres with different diameters were compared to investigate the influence of the size on the drug release kinetics. The drug contents and encapsulation efficiencies of PLGA microspheres with different diameters are listed in Table 3. Normally, the drug content and encapsulation efficiency de-

370

371

372

373

374

375

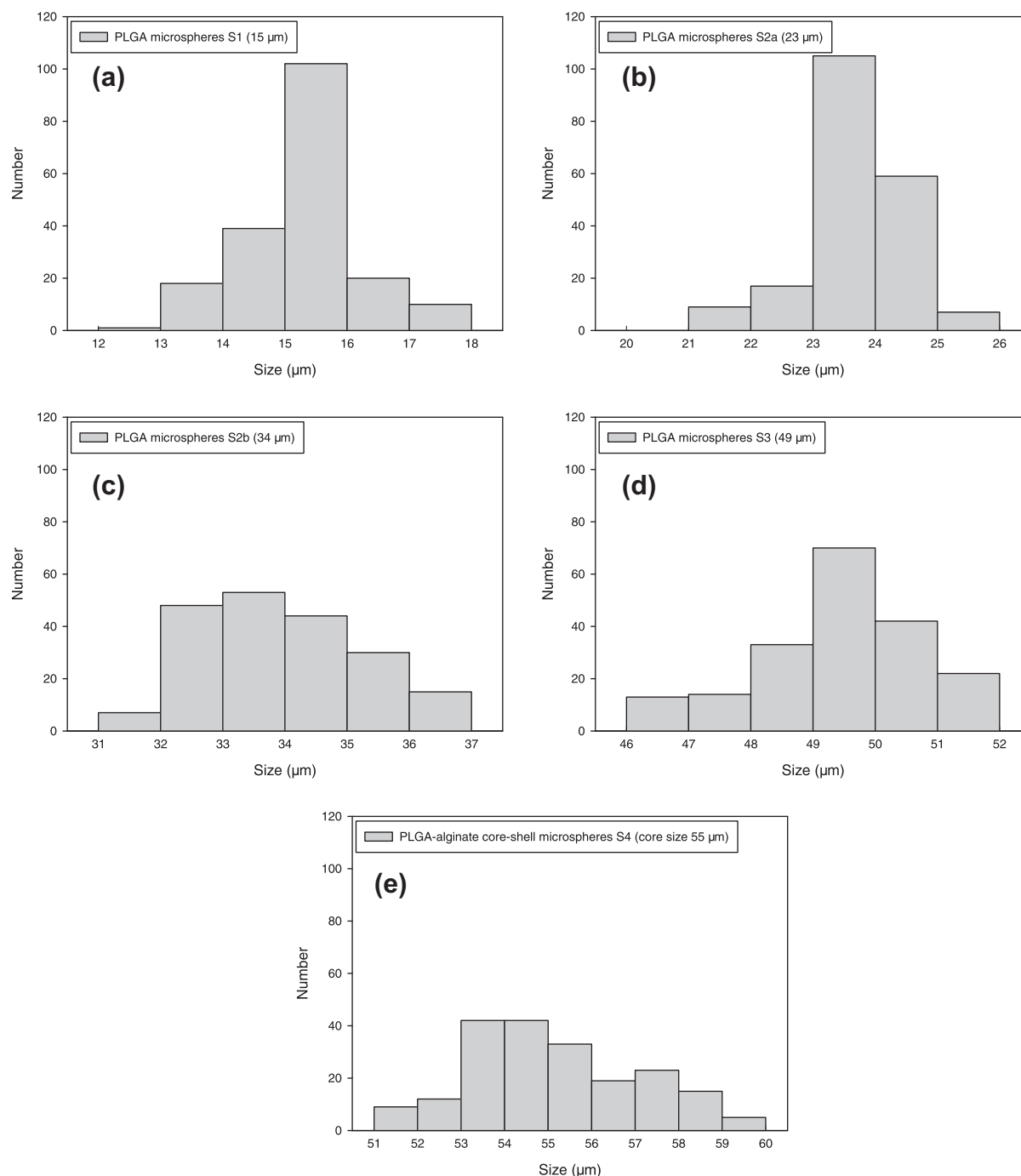


Fig. 5. Size distributions of PLGA microspheres: (a) S1, 15 μm, (b) S2a, 23 μm, (c) S2b, 34 μm and (d) S3, 49 μm. PLGA cores of PLGA–alginate core–shell microspheres: (e) S4, 55 μm.

creased with the diameter of microspheres. However, the smallest PLGA microspheres (S1) showed a relatively higher drug content and encapsulation efficiency. The major loss of rifampicin takes place during the step of evaporation, when rifampicin diffuses into the surrounding water [11]. Therefore, smaller microspheres exhibited lower encapsulation efficiency due to the relatively larger surface-to-volume ratio facilitating the diffusion of rifampicin. At the same time, larger surface-to-volume ratios may also enhance the diffusion and evaporation of DCM, and therefore shorten the duration of the evaporation process. This may be the reason that the smallest PLGA microspheres showed relatively higher drug encapsulation efficiency.

Table 3

The drug contents and encapsulation efficiencies of PLGA microspheres with different diameters.

	No.			
	S1	S2a	S2b	S3
Diameters (μm)	15.2 ± 0.7	23.6 ± 0.9	34.2 ± 1.7	49.2 ± 1.6
Drug content (%)	3.22 ± 0.11	1.70 ± 0.13	2.34 ± 0.20	4.26 ± 0.54
EE ^a (%)	35.35 ± 1.29	18.68 ± 1.43	25.68 ± 2.23	46.78 ± 5.89

^a EE: encapsulation efficiency.

The initial burst releases and in vitro release profiles of PLGA microspheres with different diameters are given in Fig. 6. Larger

PLGA microspheres (S2b and S3) exhibited significantly reduced initial burst compared with smaller PLGA microspheres (S1 and S2a). The in vitro drug release characteristics of PLGA microspheres loaded with rifampicin were presented as accumulative percentage release within 1 month (Fig. 6b). PLGA microspheres in different diameters exhibited similar sigmoid release patterns composed of three phases. Phase I was the lag phase, since the drug release rate was low in the first few days. Phase II was characterized by an upturn in the curve due to the increase of the drug release rate. In phase III, the drug release rate began to decrease so that the curve bent down. Although the drug release patterns were similar, smaller microspheres (S1 and S2a) had shorter lag phases (4 days) and larger microspheres (S2b and S3) had longer lag phases (13 days). Furthermore, all microspheres had a similar duration of phase II, which is about 9 days. Last, all microspheres entered phase III when 50–60% of the encapsulated rifampicin had been released. The drug release rates were obtained by calculating the released rifampicin (w/w%) for the same period of time, and the results are shown in Fig. 6c. It should be noted that the drug release profiles are also influenced by other factors such as the composition of PLGA. This study only focused on the influences of the microstructure of drug delivery devices.

By comparing monodisperse PLGA microspheres with different diameters, a better understanding of the drug release mechanisms of PLGA could be acquired. The results illustrate that larger microspheres had higher drug contents and drug encapsulation efficiencies. In general, the major loss of rifampicin takes place at the evaporation process, during which rifampicin diffuses into the continuous phase [11]. As a result, larger microspheres had slower diffusion rates due to the longer diffusion routes and smaller surface-to-volume ratios. However, the smallest PLGA microspheres (S1) exhibited a relatively higher drug content and encapsulation efficiency. One possible reason for this is that smaller microspheres have larger surface-to-volume ratios, which can promote the evaporation of the DCM. As a result, S1 solidified much faster than other microspheres and the time period for drug diffusion was shortened.

It was found that S1 and S2a showed a high similarity in their drug release profiles, although their drug contents were significantly different. The same situation was also found between S2b and S3. The reason for this may be that the drug contents of all groups were relatively low (less than 5%). Therefore, the influence of the drug content on the drug release kinetics could be ignored in this study. The sigmoid release pattern was common among PLGA based drug delivery devices. It is widely accepted that the drug release during phase I (the lag phase) is mainly caused by diffusion, so the drug release rate is low. In phase II, the drug release rate increased because of the erosion of PLGA. After that, the drug release

rate decreased again due to the depletion of the drug, so phase III can be seen in the curve. In this study, it was found that the lag phases of smaller microspheres were shorter than those of larger microspheres. PLGA undergoes bulk erosion rather than surface erosion, so the erosion rate would not change with size; thus the increase in the drug release rate of smaller microspheres at the early stage of phase II cannot be attributed to polymer erosion. One possible reason is that smaller PLGA microspheres undergo more severe disentanglement of polymer chains at an early stage of the drug release. It has been reported that water can decrease the glass transition temperature (T_g) of PLGA below the value at which in vitro drug release testing is usually carried out (i.e. 37 °C) [39]. This suggests that the disentanglement of polymer chains takes place after immersing in water at 37 °C. However, more studies are required to fully understand this phenomenon. Interestingly, all PLGA microspheres showed similar lengths of phase II, and the changes in drug release rates during phase II were similar (Fig. 6c). Furthermore, PLGA microspheres with all diameters entered the phase when 50–60% of the encapsulated rifampicin had been released. This suggests that, for the PLGA used in this study, the time points at which the PLGA microspheres entered phase II and phase III were in fact controlled by the size.

To conclude, the size of PLGA microspheres plays an important role in the drug release kinetics. Smaller PLGA microspheres have a reduced initial burst and a shorter lag phase, which facilitates the control of the drug release kinetics. The size also determines when the PLGA microspheres enter phase II and phase III. With the capillary microfluidic method, one can delicately control the drug release kinetics by fabricating monodisperse microspheres with controlled size.

3.4. Influences of the core-shell structure on the drug release kinetics

The influences of the shells were investigated by comparing PLGA microspheres (S3) and PLGA-alginate core-shell microspheres (S4). The core size of PLGA-alginate core-shell microspheres ($55.1 \pm 4.5 \mu\text{m}$) was similar to that of the PLGA microspheres ($49.2 \pm 1.6 \mu\text{m}$). The core-shell microspheres exhibited higher drug content ($6.41 \pm 0.03\%$) and enhanced drug encapsulation efficiency ($70.47 \pm 1.85\%$).

The drug release characteristics of PLGA microspheres and PLGA-alginate core-shell microspheres were compared in Fig. 7. PLGA-alginate core-shell microspheres had lower initial burst release (Fig. 7a). As shown in Fig. 7b, PLGA-alginate core-shell microspheres also showed a lag phase which was similar to PLGA microspheres. However, instead of phase II and phase III, a near-zero-order release was observed from PLGA-alginate core-shell microspheres after phase I.

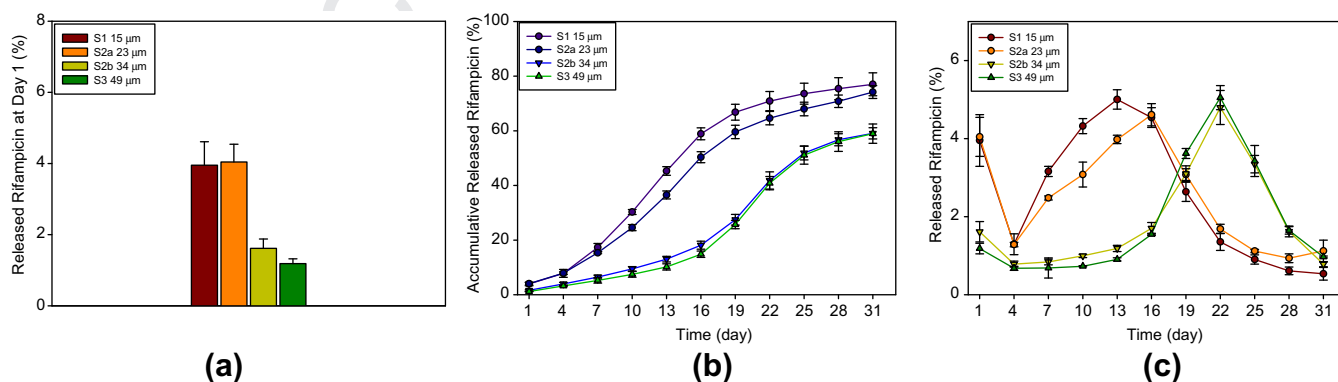


Fig. 6. Drug release characteristics of PLGA microspheres with different diameters: (a) initial burst releases, (b) in vitro drug release profiles and (c) drug release rates. *Significant difference ($p < 0.05$).

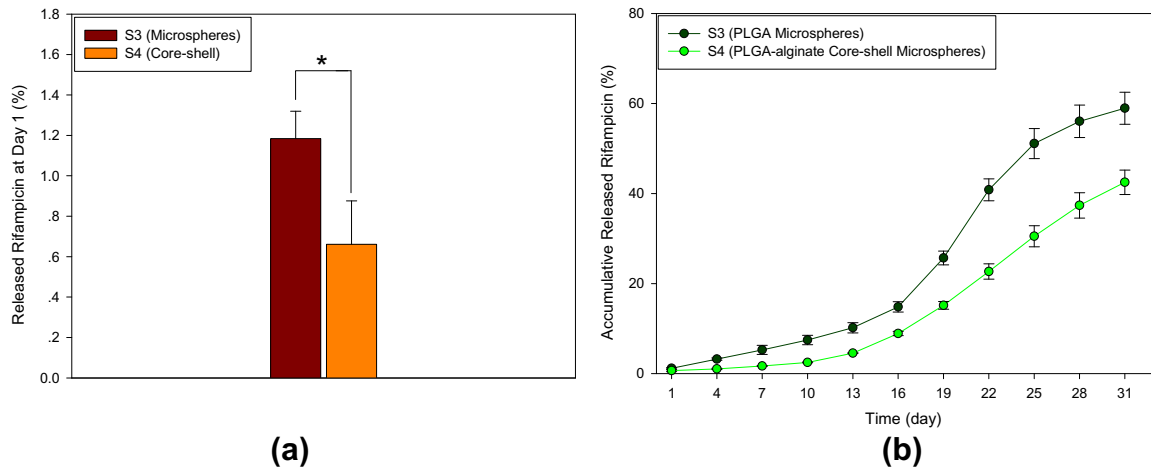


Fig. 7. Drug release characteristics of PLGA microspheres (S3, 49 μm) and PLGA-alginate core-shell microspheres (S4, 55 μm): (a) initial burst releases, (b) in vitro release of PLGA microspheres and PLGA-alginate core-shell microspheres. *Significant difference ($p < 0.05$).

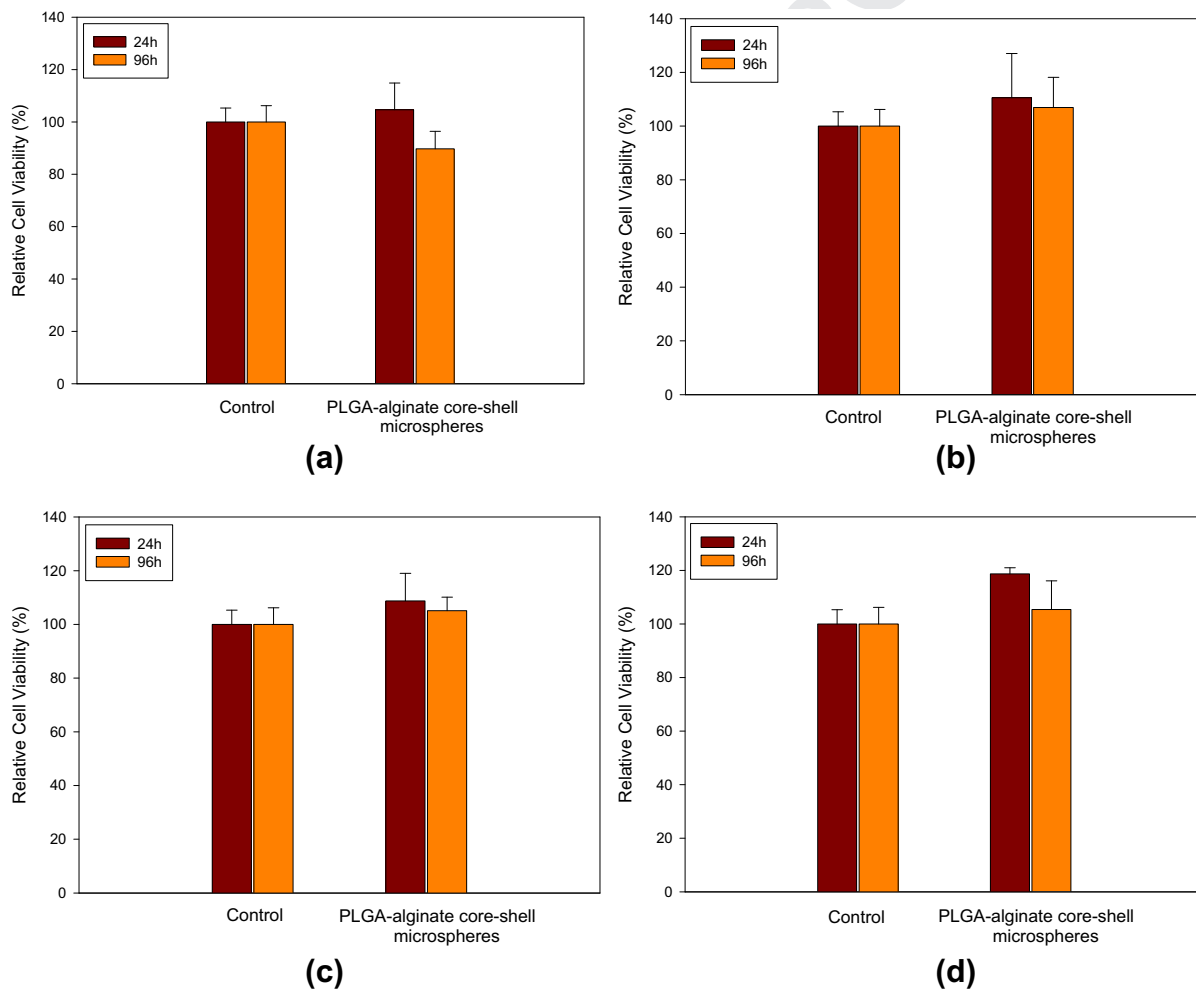


Fig. 8. Relative cell viability (%) of PLGA-alginate core-shell microspheres: (a) 100% extraction, (b) 50% extraction, (c) 25% extraction and (d) 12.5% extraction.

During the fabrication process, the shell layer was solidified before the evaporation of solvent. The diffusion of the drug during the solvent evaporation was reduced by the shell layer due to the shell being a physical barrier, and the encapsulation efficiency was increased. In the core-shell structure, the loaded rifampicin was first

released from the PLGA core and then diffused through the shell into the environment. The diffusion of the drug should be slower in the alginate shell than in the pure solutions. Therefore, the overall drug release rate was retarded by the alginate shell. During the lag phase, the drug release rate of the PLGA core was low so that

the overall drug release rate of the PLGA–alginate core–shell microspheres was mainly controlled by the PLGA core. However, when the drug release rate of the PLGA core increased, the shells acted as buffer layers and the overall drug release rate was mainly controlled by the diffusion in the shell layers. As a result, a near-zero-order release was achieved.

To sum up, the shell layer can increase the drug encapsulation efficiency and modulate the drug release kinetics. When the drug release rate of the PLGA core is high enough, the shell layer will act as a buffer layer and a near-zero-order release can be achieved. The capillary microfluidic method is a powerful tool to control the drug release kinetics by both controlling the size of PLGA cores and fabricating homogeneous shells on PLGA cores.

3.5. Biocompatibility

The biocompatibility of the PLGA–alginate core–shell microspheres was characterized by relative cell viability from MTT assay. According to the results (Fig. 8), no significant difference was found in L929 mouse fibroblasts cell viability between control group and PLGA–alginate core–shell microspheres group at both 24 and 96 h. PLGA–alginate core–shell microspheres gave low or no cytotoxicity, even at highest concentration (Fig. 8a), since cell viabilities were all more than 80% [40].

Biocompatibility is one of the most important issues for biomaterials in long-term applications. The excellent biocompatibility of PLGA has been well accepted after years of study [8,41]. Alginate has been used as a cell carrier and wound dressing and no obvious toxicity was reported [42,43]. However, it is still necessary to find out the toxic effect, if any, of the PLGA–alginate core–shell microspheres fabricated by the method presented in this study. The MTT assay results suggested that PLGA–alginate core–shell microspheres fabricated by the capillary microfluidic method is biocompatible and can be a potential device for controlled drug release.

4. Conclusion

Monodisperse PLGA–alginate core–shell microspheres with controlled size and homogeneous shells were first fabricated using capillary microfluidic devices. The size of the PLGA cores was readily controlled by the geometries of the capillary microfluidic devices and the fluid flow rates. It was also found that increasing the size of the PLGA microspheres could reduce the initial burst release and lengthen the lag phase. Furthermore, the time points at which the PLGA microspheres entered phase II and phase III were controlled by size. By fabricating PLGA–alginate core–shell microspheres using the capillary microfluidic method, one could increase the encapsulation efficiency and reduce the initial burst release. The shell layer could also modulate the drug release kinetics. When the drug release rate of the core was high enough, the shell would act as a buffer layer so that a near-zero-order release pattern was achieved.

The monodisperse PLGA–alginate core–shell microspheres with controlled size and homogeneous shells fabricated by the capillary microfluidic method can provide tunable drug release kinetics. The drug release kinetics can be modulated by the shell layer and the PLGA core size. Furthermore, the PLGA–alginate core–shell microspheres were biocompatible. These properties make it a promising device for controlled drug release.

Acknowledgements

We gratefully acknowledge financial support from the Research Grants Council of Hong Kong (GRF718009, GRF718111 and HKU707712P), the Science and Technology Innovation Commis-

sion of Shenzhen Municipality (JC201105190878A), National Natural Science Foundation of China (NSFC51206138/E0605) and the Seed Funding from The University of Hong Kong (201109160030 and 201109176165). This research is supported in part by the Zhejiang Provincial, Hangzhou Municipal and Lin'an County Governments.

Appendix A. Figures with essential colour discrimination

Certain figures in this article, particularly Figs. 1–4 and 6–8 are difficult to interpret in black and white. The full colour images can be found in the on-line version, at <http://dx.doi.org/10.1016/j.actbio.2013.03.022>.

References

- Langer R. Polymer-controlled drug delivery systems. *Acc Chem Res* 1993;26:537–42.
- Allen T, Cullis P. Drug delivery systems: entering the mainstream. *Science* 2004;303:1818–22.
- Uhrich K, Cannizzaro S, Langer R, Shakesheff K. Polymeric systems for controlled drug release. *Chem Rev* 1999;99:3181–98.
- Malam Y, Loizidou M, Seifalian AM. Liposomes and nanoparticles: nanosized vehicles for drug delivery in cancer. *Trends Pharmacol Sci* 2009;30:592–9.
- Zhang J, Misra R. Magnetic drug-targeting carrier encapsulated with thermosensitive smart polymer: core-shell nanoparticle carrier and drug release response. *Acta Biomater* 2007;3:838–50.
- Yuan Q, Shah J, Hein S, Misra R. Controlled and extended drug release behavior of chitosan-based nanoparticle carrier. *Acta Biomater* 2010;6:1140–8.
- Bae SE, Son JS, Park K, Han DK. Fabrication of covered porous PLGA microspheres using hydrogen peroxide for controlled drug delivery and regenerative medicine. *J Control Release* 2009;133:37–43.
- Anderson JM, Shive MS. Biodegradation and biocompatibility of PLA and PLGA microspheres. *Adv Drug Deliv Rev* 2012;64:72–82.
- Crielaard BJ, van der Wal S, Le HT, Bode ATL, Lammers T, Hennink WE, et al. Liposomes as carriers for colchicine-derived prodrugs: vascular disrupting nanomedicines with tailorable drug release kinetics. *Eur J Pharm Sci* 2011;45:429–35.
- Klose D, Siepmann F, Elkharraz K, Krenzlin S, Siepmann J. How porosity and size affect the drug release mechanisms from PLGA-based microparticles. *Int J Pharm* 2006;314:198–206.
- Budhian A, Siegel SJ, Winey KI. Haloperidol-loaded PLGA nanoparticles: systematic study of particle size and drug content. *Int J Pharm* 2007;336:367–75.
- Berkland C, King M, Cox A, Kim K, Pack D. Precise control of PLG microsphere size provides enhanced control of drug release rate. *J Control Release* 2002;82:137–47.
- Dawes GJS, Fratila-Apachitei L, Mulia K, Apachitei I, Witkamp GJ, Duszczak J. Size effect of PLGA spheres on drug loading efficiency and release profiles. *J Mater Sci – Mater Med* 2009;20:1089–94.
- Whitesides GM. The origins and the future of microfluidics. *Nature* 2006;442:368–73.
- Utada A, Lorenceau E, Link D, Kaplan P, Stone H, Weitz DA. Monodisperse double emulsions generated from a microcapillary device. *Science* 2005;308:537–41.
- De Geest BG, Urbanski JP, Thorsen T, Demeester J, De Smedt SC. Synthesis of monodisperse biodegradable microgels in microfluidic devices. *Langmuir* 2005;21:10275–9.
- Kim JW, Utada AS, Fernández-Nieves A, Hu Z, Weitz DA. Fabrication of monodisperse gel shells and functional microgels in microfluidic devices. *Angew Chem* 2007;119:1851–4.
- Shum HC, Kim JW, Weitz DA. Microfluidic fabrication of monodisperse biocompatible and biodegradable polymersomes with controlled permeability. *J Am Chem Soc* 2008;130:9543–9.
- Liu K, Ding HJ, Liu J, Chen Y, Zhao XZ. Shape-controlled production of biodegradable calcium alginate gel microparticles using a novel microfluidic device. *Langmuir* 2006;22:9453–7.
- Tran TH, Nguyen CT, Kim DP, Lee Y, Huh KM. Microfluidic approach for highly efficient synthesis of heparin-based bioconjugates for drug delivery. *Lab Chip* 2012;12:589–94.
- Champion J, Katare Y, Mitragotri S. Particle shape: a new design parameter for micro- and nanoscale drug delivery carriers. *J Control Release* 2007;121:3–9.
- Xu Q, Hashimoto M, Dang TT, Hoare T, Kohane DS, Whitesides GM, et al. Preparation of monodisperse biodegradable polymer microparticles using a microfluidic flow-focusing device for controlled drug delivery. *Small* 2009;5:1575–81.
- Duncanson WJ, Zieringer M, Wagner O, Wilking JN, Abbaspourrad A, Haag R, et al. Microfluidic synthesis of monodisperse porous microspheres with size-tunable pores. *Soft Matter* 2012;8:10636–40.

- 628 [24] Hu C, Feng H, Zhu C. Preparation and characterization of rifampicin–PLGA
629 microspheres/sodium alginate in situ gel combination delivery system.
630 Colloids Surf, B 2012;95:162–9.
- 631 [25] Choi DH, Park CH, Kim IH, Chun HJ, Park K, Han DK. Fabrication of core–shell
632 microcapsules using PLGA and alginate for dual growth factor delivery system.
633 J Control Release 2010;147:193–201.
- 634 [26] Okushima S, Nisisako T, Torii T, Higuchi T. Controlled production of
635 monodisperse double emulsions by two-step droplet breakup in microfluidic
636 devices. Langmuir 2004;20:9905–8.
- 637 [27] Zhang J, Wang Q, Wang A. In situ generation of sodium alginate/
638 hydroxyapatite nanocomposite beads as drug-controlled release matrices.
639 Acta Biomater 2010;6:445–54.
- 640 [28] Murata Y, Sasaki N, Miyamoto E, Kawashima S. Use of floating alginate gel
641 beads for stomach-specific drug delivery. Eur J Pharm Biopharm
642 2000;50:221–6.
- 643 [29] Shah RK, Shum HC, Rowat AC, Lee D, Agresti JJ, Utada AS, et al. Designer
644 emulsions using microfluidics. Mater Today 2008;11:18–27.
- 645 [30] Beck-Broichsitter M, Schweiger C, Schmehl T, Gessler T, Seeger W, Kissel T.
646 Characterization of novel spray-dried polymeric particles for controlled
647 pulmonary drug delivery. J Control Release 2012;158:329–35.
- 648 [31] Dutt M, Khuller G. Chemotherapy of Mycobacterium tuberculosis infections in
649 mice with a combination of isoniazid and rifampicin entrapped in poly(DL-
650 lactide-co-glycolide) microparticles. J Antimicrob Chemother
651 2001;47:829–35.
- 652 [32] Blanchemain N, Laurent T, Chai F, Neut C, Haulon S, Krump-Konvalinkova V,
653 et al. Polyester vascular prostheses coated with a cyclodextrin polymer and
654 activated with antibiotics: cytotoxicity and microbiological evaluation. Acta
655 Biomater 2008;4:1725–33.
- 656 [33] Ignatius A, Claes LE. In vitro biocompatibility of bioresorbable polymers: poly(L,
657 DL-lactide) and poly(L-lactide-co-glycolide). Biomaterials 1996;17:831–9.
- [34] Ozdemir KG, Yilmaz H, Yilmaz S. In vitro evaluation of cytotoxicity of soft
658 lining materials on L929 cells by MTT assay. J Biomed Mater Res B Appl
659 Biomater 2009;90:82–6.
- [35] Zange R, Li Y, Kissel T. Biocompatibility testing of ABA triblock copolymers
660 consisting of poly(L-lactic-co-glycolic acid) A blocks attached to a central
661 poly(ethylene oxide) B block under in vitro conditions using different L929
662 mouse fibroblasts cell culture models. J Control Release 1998;56:249–58.
- [36] Yang J, Lee C-H, Park J, Seo S, Lim E-K, Song YJ, et al. Antibody conjugated
663 magnetic PLGA nanoparticles for diagnosis and treatment of breast cancer. J
664 Mater Chem 2007;17:2695–9.
- [37] Paragkumar NT, Edith D, Six J-L. Surface characteristics of PLA and PLGA films.
665 Appl Surf Sci 2006;253:2758–64.
- [38] Papageorgiou SK, Kouvelos EP, Favvas EP, Sapalidis AA, Romanos GE, Katsaros
666 FK. Metal–carboxylate interactions in metal–alginate complexes studied with
667 FTIR spectroscopy. Carbohydr Res 2010;345:469–73.
- [39] Passerini N, Craig D. An investigation into the effects of residual water on the
668 glass transition temperature of polylactide microspheres using modulated
669 temperature DSC. J Control Release 2001;73:111–5.
- [40] Mahmoudi M, Simchi A, Milani A, Stroeve P. Cell toxicity of superparamagnetic
670 iron oxide nanoparticles. J Colloid Interface Sci 2009;336:510–8.
- [41] Shi G, Cai Q, Wang C, Lu N, Wang S, Bei J. Fabrication and biocompatibility of
671 cell scaffolds of poly(L-lactic acid) and poly(L-lactic-co-glycolic acid). Polym
672 Adv Technol 2002;13:227–32.
- [42] Eiselt P, Yeh J, Latvala RK, Shea LD, Mooney DJ. Porous carriers for biomedical
673 applications based on alginate hydrogels. Biomaterials 2000;21:1921–7.
- [43] Borges O, Cordeiro-da-Silva A, Romeijn SG, Amidi M, De Sousa A, Borchard G,
674 et al. Uptake studies in rat Peyer's patches, cytotoxicity and release studies of
675 alginate coated chitosan nanoparticles for mucosal vaccination. J Control
676 Release 2006;114:348–58.
- 677
678
679
680
681
682
683
684
685
686
687